

# Synthesis and charge–discharge properties of a ferrocene-containing polytriphenylamine derivative as the cathode of a lithium ion battery

Chang Su, Yinpeng Ye, Lihuan Xu and Cheng Zhang\*

Received 19th July 2012, Accepted 7th September 2012

DOI: 10.1039/c2jm34752k

In this work, a novel linear polytriphenylamine derivative was successfully synthesized by the introduction of ferrocene as a terminating group to the triphenylamine moieties. The morphology, structure and charge–discharge performance of the prepared polymer as the cathode were characterized by fourier transform infrared spectroscopy (FTIR), ultraviolet visible spectroscopy (UV-vis), scanning electron microscopy (SEM), cyclic voltammograms (CV) and galvanostatic charge–discharge testing. The results showed that the introduction of ferrocene to polytriphenylamine obviously improved the specific capacity and rate capability of the resulting PTPAFc cathodes in lithium ion batteries. Under our experimental conditions, the PTPAFc-based electrodes exhibited an initial discharge capacity of up to 100.2 mA h g<sup>-1</sup> at 20 mA g<sup>-1</sup> between 2.5 and 4.2 V, while PTPAn-based electrodes only presented 70.3 mA h g<sup>-1</sup>, comparatively. Also, the PTPAFc cathode specially retained over 89.7% of the initial capacity with a ten times increase of the current from 50 to 500 mA g<sup>-1</sup>. These improved electrochemical performances were ascribed to the introduction of ferrocene as the termination couple, which makes the PTPAFc main chain as a chainlike molecule structure and benefits from charge carrier transportation in the molecular polymer.

## 1. Introduction

Li-ion batteries as a promising power source have received widespread attention, owing to their convenient and good charge–discharge capacity.<sup>1–4</sup> However, current Li-ion battery technologies are mostly based on transition-metal cathodes (such as LiCoO<sub>2</sub>, LiMnO<sub>2</sub> and V<sub>2</sub>O<sub>5</sub>), which have serious cost and resource limitations that hinder their large scale application for upcoming portable electronic devices.<sup>5–8</sup> A variety of efforts have been undertaken to improve the battery materials, such as using nanosized and nanostructured materials, doping transition-metal cathodes, optimizing the electrode components and developing novel cathodic materials, *etc.* Among all of the attempts, the application of organic electronics materials as cathode materials in Li-ion batteries has been explored because of easy preparation and high energy density. So far several types of organic positive-electrode materials have been proposed, mainly including electroactive conducting polymers,<sup>8,9</sup> organo-sulfur polymers,<sup>10</sup> nitroxide radical tetramethylpiperidine-*N*-oxyl (TEMPO)-based polymers,<sup>11,12</sup> pendant-type polymer based on ferrocene and carbazole,<sup>13,14</sup> aromatic carbonyl derivatives and quinine-based materials,<sup>15</sup> *etc.* All of these make the

performances of organic-based cathodes of lithium ion batteries improve constantly.

Among the above organic positive-electrode materials, the polymers with organic redox radicals as the stable backbone or pendant groups have attracted much interest of researchers.<sup>11,12,16</sup> Among the radicals polymers, polytriphenylamine (PTPAn) and related derivatives are well known as p-type conductors and have been widely applied as organic electroluminescence (EL) materials and photo-conduction materials.<sup>17</sup> Recently, the triphenylamine-based radical polymer material has also been explored in the energy storage field, such as lithium ion batteries<sup>16</sup> and super capacitors,<sup>18</sup> and exhibits excellent electrochemical property. As reported,<sup>16</sup> PTPAn, which is composed of a  $\pi$ -conjugated triphenylamine substructure, showed good electrochemical performance and well-defined voltage plateaus ( $\sim 3.6$  V) as the cathode of lithium ion batteries. However, the steric torsion of neighbouring molecules in PTPAn molecular chains limits effective electron transportation during the redox process, resulting in poor electron/ion conductivity in the polymer. In addition, the serious crosslinking structure of PTPAn, due to three polymerizable active sorts of triphenylamine unit, will make an aggregation of PTPAn particles and this hinders the electrolyte to infiltrate to the surface of PTPAn. As a result, the active parts of PTPAn will not be fully utilized, and the high cell performance cannot be fully reached. As a solution, producing a linear structure of PTPAn will be an effective way to relieve steric torsion in PTPAn molecular chains and decrease the crosslinking density of PTPAn, which, as a result, will promote the electrolyte

State Key Laboratory Breeding Base of Green Chemistry Synthesis Technology, International Science and Technology Cooperation Base of Energy Materials and Application, College of Chemical Engineering and Materials Science, Zhejiang University of Technology, Hangzhou, 310014, P. R. China. E-mail: czhang@zjut.edu.cn; Tel: +86-571-88320253

to approach the redox active center of PTPAn and improve the cell performance of PTPAn-based cathodes.

Ferrocene as an organometallic compound has been extensively investigated as a standard electrode in redox potential measurements because of its air stability, excellent electrochemical response, redox property, and so on.<sup>19–22</sup> It has been reported<sup>13</sup> that polymers carrying ferrocene moieties such as poly(vinylferrocene), poly(ethynylferrocene) and poly(ferrocene) have been applied to cathode-active materials in organic lithium ion batteries, which exhibit promising battery properties, such as being quickly chargeable, having a high power density and the stable voltage plateaus ( $\sim 3.4$  V) as PTPAn. In light of these considerations, we utilized the ferrocene as the terminating group to terminate one of three polymerizable active sorts of triphenylamine precursors, then a linear polymer based on the prepared ferrocene-contained polytriphenylamine monomer was synthesized by a chemical polymerization method. Thanks to the un-crosslinking structure of the novel linear polymer and the introduction of the electroactive ferrocene as the active terminating group, the prepared ferrocene-contained polytriphenylamine polymer as the cathode of organic lithium ion battery exhibited an improved discharge specific capability and superior rate capability by using the lithium ion half-cell method, compared to that of the conventional PTPAn, which was promising for advanced cathode materials.

## 2. Experimental

### Material synthesis

**Monomer.** 4-nitro-*N,N*-diphenylaniline (1) was synthesized as following: *N*-phenylaniline (1.69 g) and sodium hydride (0.9 g) were firstly dissolved in 30 mL of *N,N*-dimethylacetamide (DMAC). Then, 4-fluoronitrobenzene (2.11 g) was added into the above solution. The reaction was carried out under a nitrogen atmosphere for 4 h. The resulting solution was extracted with chloroform and dried by anhydrous  $MgSO_4$ . The obtained 4-nitro-*N,N*-diphenylaniline (1) was isolated by column chromatography with 81% yield as a yellow residue. <sup>1</sup>H NMR ( $CDCl_3$ , 400 MHz)  $\delta$  ppm<sup>-1</sup>: 6.94 (d, 2H), 7.20 (d, 4H), 7.25 (d, 2H), 7.39 (t, 4H), 8.05(d, 2H).

*N,N'*-diphenylbenzene-1,4-diamine (2) was synthesized as following: reduced iron powder (0.8 g) and ammonium chloride (1.4 g) were dispersed in a mixed solution of ethanol (50 mL) and water (50 mL). To the above dispersed solution, 1.5 g of 4-nitro-*N,N*-diphenylaniline was then added. The reaction mixture was refluxed for 2 h under a nitrogen atmosphere. The reaction mixture was then cooled, and the excess iron powder was filtered off. The solution was extracted with chloroform and dried over anhydrous  $MgSO_4$ . *N,N'*-diphenylbenzene-1,4-diamine (2) was isolated by column chromatography in 89% yield as a purple residue. <sup>1</sup>H NMR ( $CDCl_3$ , 400 MHz)  $\delta$  ppm<sup>-1</sup>: 4.10 (s, 2H, broad,  $NH_2$ ), 6.72 (d, 2H), 6.94 (t, 2H), 6.99 (d, 2H), 7.05 (d, 4H), 7.22 (t, 4H).

(*E*)-*N*-(4-(Diphenylamino)phenyl)formimidoyl ferrocene (TPAFc) was synthesized as follows: *N,N'*-diphenylbenzene-1,4-diamine (0.69 g) and ferrocenecarboxaldehyde (0.53 g) were dissolved in 30 mL of ethanol (100 mL) and refluxed for 3 h. After evaporation of ethanol, TPAFc was isolated by column

chromatography as an orange residue with 62.9% yield. <sup>1</sup>H NMR ( $CDCl_3$ , 400 MHz)  $\delta$  ppm<sup>-1</sup>: 4.26 (s, 5H, ferrocene), 4.50 (s, 2H, ferrocene), 4.81 (s, 2H, ferrocene), 7.02 (t, 2H), 7.11 (d, 8H), 7.26 (t, 4H), 8.38 (s, 1H). MS (EI):  $m/z = 456.2$  ( $M^+$ ).

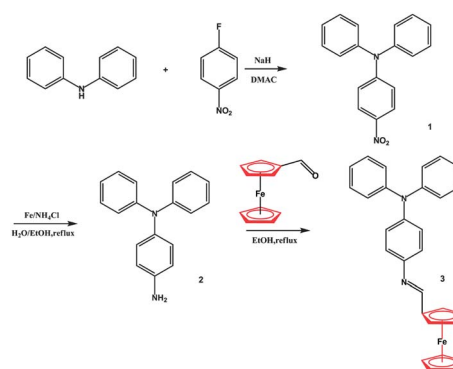
**Polymer.** The polymer of TPAFc was prepared by chemical oxidative polymerization of TPAFc in chloroform (20 ml) using ferric chloride as the oxidant. The solution was stirred over night at room temperature under  $N_2$ . After completion of the solution polymerization reaction, the reaction mixture was poured into methanol to deposit the polymer product, which was then filtered and washed with methanol several times. Finally, the polymer product was filtered and dried in vacuum at 50 °C for 12 h. The chemical structure of the polymer is shown in Scheme 1.

### Material characterization

FT-IR spectra were carried out on a Nicolet 6700 spectrometer (Thermo Fisher Nicolet, USA) with KBr pellets. UV-vis spectra were recorded on a Varian Cary 100 UV-vis spectrophotometer (Varian, USA), and the measurement was carried out in DMF solution. <sup>1</sup>H NMR spectra of the compounds were recorded on a Bruker AVANCE III 500 MHz spectrometer (Bruker, Switzerland) using  $CDCl_3$ . The mass spectrometry (MS) analysis was measured on a GCT Premier spectrometer (Waters, USA) using the electron impact (EI<sup>+</sup>) mass spectra technique. Scanning electron microscopy (SEM) measurements were taken using a Hitachi S-4800 scanning electron microscope (Hitachi, Japan).

### Electrochemical measurements

For cathode characterization, CR2032 coin-type cell was used and assembled in an argon-filled glove box. The cathode electrodes were prepared by coating a mixture containing 50% as prepared polymers, 40% acetylene black, 10% PVDF binder on circular Al current collector foils, followed by drying at 60 °C for 10 h. After that, the cells were assembled with lithium foil as the anode, the prepared electrodes as the cathode and 1 M LiPF<sub>6</sub> dissolved in ethylenecarbonate (EC) and dimethylcarbonate (DMC) (EC/DMC = 1 : 1 v/v) as the electrolyte. The charge–discharge measurements were carried out on a LAND CT2001A in the voltage range of 2.5–4.2 V *versus* Li/Li<sup>+</sup>, using a constant current density at room temperature. The cyclic voltammograms (CV) tests was performed with a CHI 660C electrochemical



**Scheme 1** The synthesis route to TPAFc.

working station in 0.1 M  $[\text{Bu}_4\text{N}]\text{ClO}_4\text{-CH}_2\text{Cl}_2$  versus  $\text{Ag}/\text{AgCl}$  at a scan rate of  $25 \text{ mV s}^{-1}$ .

### 3. Results and discussion

#### 3.1. Material characterization

**FTIR.** Fig. 1 shows the FTIR spectra of the as-prepared PTPAn and PTPAFc. As shown in Fig. 1, the main characteristic peaks of the triphenylamine moieties can be found in the two samples for the C=C ring stretching at  $1590 \text{ cm}^{-1}$ , C-C stretching at  $1494 \text{ cm}^{-1}$  and C-H bending at  $1590$  and  $1494 \text{ cm}^{-1}$ . Also, the absorption peaks at  $1276$  and  $820 \text{ cm}^{-1}$  correspond to the C-N stretching from the tertiary amine and a C-H out-of-plane vibration from 1,4-disubstituted benzene rings.<sup>16</sup> Besides, some new bands can be observed clearly in the spectrum of PTPAFc. The absorption peaks at  $1631 \text{ cm}^{-1}$  can be ascribed to the N=C (Schiff base structure) stretching. The absorption peaks at  $1103$ ,  $827$  and  $474 \text{ cm}^{-1}$  are due to the mono-substituted ferrocene.<sup>23,24</sup> These indicate that the PTPAFc polymer contains both triphenylamine and ferrocene moieties.

**UV-vis.** The UV-vis spectra (normalized absorbance) are further utilized to explore the characteristics of the TPAFc monomer and PTPAFc, comparatively. As shown in Fig. 2, the TPAFc monomer exhibits two pairs of absorption peaks, at  $293 \text{ nm}$  and  $362 \text{ nm}$ , respectively. The maximum at  $362 \text{ nm}$  is assigned to the  $\pi\text{-}\pi^*$  electron transition from the triphenylamine units of TPAFc,<sup>16,23</sup> while the absorption peaks at  $\sim 293 \text{ nm}$  correspond to the  $\pi\text{-}\pi^*$  electron transition of the ferrocene moieties. After the chemical polymerization, it can be seen that the corresponding absorption peaks for the obtained PTPAFc are obviously red-shifted to  $305 \text{ nm}$  and about  $450 \text{ nm}$ , respectively, in comparison with that of the TPAFc monomer, which is due to the expansion of the  $\pi$ -conjugated systems by the produced conjugated polymer system. As a result, the charge carrier transportation alone in the polymer main chain of PTPAn is improved, which is crucial for high-performance lithium batteries.

**SEM.** Fig. 3 shows the morphology of the PTPAn and PTPAFc. As can be seen, the PTPAn polymer has a dense packing structure and the aggregation of PTPAn particles can be noticed obviously. This structural feature may be caused by the

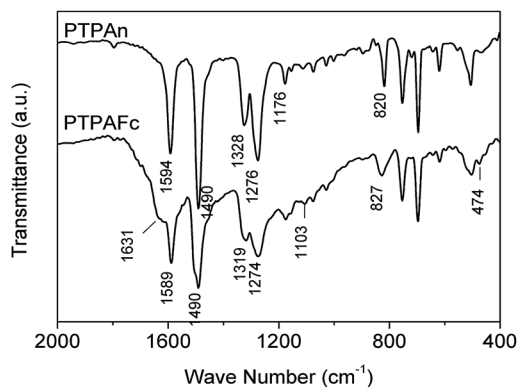


Fig. 1 FTIR spectrum of the PTPAn and PTPAFc sample.

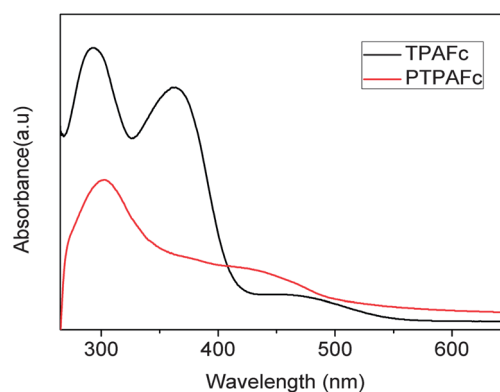


Fig. 2 UV-vis spectra of PTPAn and PTPAFc ( $10^{-3} \text{ g L}^{-1}$ ) in DMF.

steric torsion of the main chains by the big triphenylamine units. However, as the ferrocene couple is introduced to the triphenylamine, the morphology of PTPAFc is very different from that of PTPAn. As shown in Fig. 3(b), PTPAFc shows a loose assembled particle structure with a size of about  $100 \text{ nm}$ . This feature may provide sufficient surface area and ionic channels for redox reactions of a polymeric electrode.

#### 3.2. Electrochemical performance

Fig. 4 shows the cyclic voltammetry (CV) profiles of both PTPAn and PTPAFc measured in  $0.1 \text{ M } [\text{Bu}_4\text{N}]\text{ClO}_4\text{-CH}_2\text{Cl}_2$  solution. As can be seen, the electrode of PTPAn shows a couple of anodic and cathodic peaks corresponding to the charge-discharge reaction of the radical redox couple of PTPAn at about  $1.05$  and  $0.8 \text{ V}$  respectively. The potential separation between the oxidation and reduction peaks is about  $0.25 \text{ V}$ . The approximately symmetrical peaks suggest a good insertion/extraction reversibility of the produced PTPAn cathode active material. Comparably, there is some difference between the CV curves of PTPAn and PTPAFc. For PTPAFc, it exhibits one pair of well-overlapped and broad redox peaks, which can be explained as the organometallic ferrocene, the activity compound, possesses similar charge-discharge voltage plateaus as that of PTPAn, which may stack up to give broad redox peaks. Correspondingly, the oxidation redox peaks of the PTPAFc shift to  $1.03$  and  $1.16 \text{ V}$ , respectively. The peak separation exhibited by the PTPAFc electrode is about  $0.13 \text{ V}$ , which is about  $0.12 \text{ V}$  smaller than that of the PTPAn electrode, suggesting the lower degree of polarization of the PTPAFc material during the electrochemical reaction. These results are in good agreement with the electrochemical cycling performance of the PTPAFc cathode as described below.

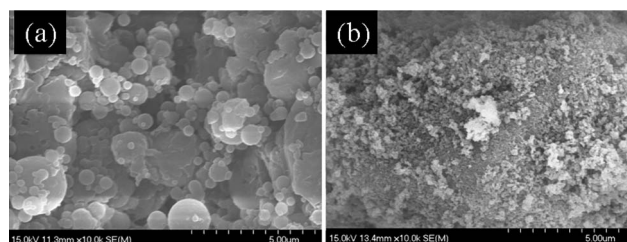
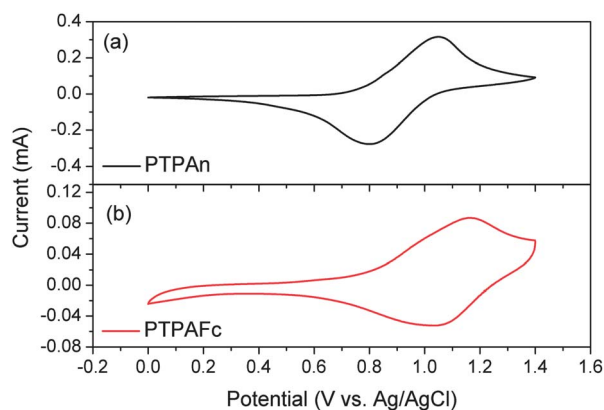


Fig. 3 SEM images of powder samples (a) PTPAn and (b) PTPAFc.



**Fig. 4** Cyclic voltammograms (CV) of (a) PTPAn and (b) PTPAFc in 0.1 M  $[\text{Bu}_4\text{N}]\text{ClO}_4\text{-CH}_2\text{Cl}_2$  versus Ag/AgCl at a scan rate of  $25 \text{ mV s}^{-1}$ .

### 3.3. Charge–discharge performance

The charge–discharge behaviours of the as-prepared polymers as cathode materials of Li-ion batteries are examined, respectively. The initial charge–discharge profiles of the polymers at  $20 \text{ mA g}^{-1}$  between 2.5 and 4.2 V in  $\text{LiPF}_6 \text{ EC/DMC}$  (v/v, 1 : 1) electrolyte are shown in Fig. 5. As it can be seen in the figure, the PTPAn shows an initial discharge capacity of  $70.3 \text{ mA h g}^{-1}$  with a typical voltage plateau in the voltage range of 3.5–4.1 V at the initial cycle. However, under the same conditions, the PTPAFc electrode exhibits an initial discharge capacity of up to  $100.2 \text{ mA h g}^{-1}$ . The improvement of the PTPAFc electrode capacity can be ascribed to higher theoretical capacities of PTPAFc ( $120.5 \text{ mA.g}^{-1}$ ) than that of PTPAn ( $109.4 \text{ mA.g}^{-1}$ ), and the produced linear structure of PTPAn by an introduction of ferrocene as the terminating group to one of three polymerizable active sorts of triphenylamine precursors, which will decrease the crosslinking density of PTPAn and promote the electrolyte to approach the redox active center of PTPAn, as a result, improving the availability of the redox active material and the cell specific capability of the PTPAn-based cathode. Furthermore, the tiny particle morphology of PTPAFc compared to that of PTPAn further facilitates the diffusion of the electrolyte solution to the active-polymer center and improves the PTPAFc performance to some degree. Otherwise, there are some

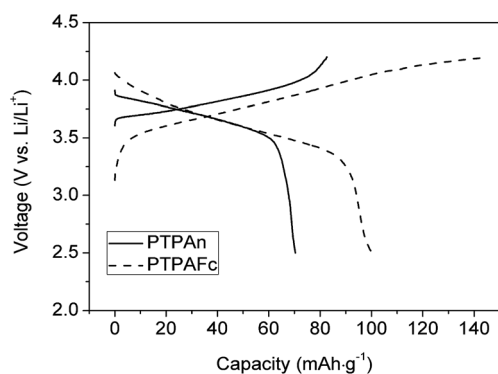


**Fig. 5** Initial charge–discharge profiles of the polymer electrodes material at a constant current of  $20 \text{ mA g}^{-1}$  between 2.5 and 4.2 V in  $\text{LiPF}_6 \text{ EC/DMC}$  (v/v, 1 : 1) electrolyte versus Li/Li<sup>+</sup>.

differences in the voltage plateau of PTPAFc and PTPAn. There are two voltage plateaus observed during the charge process in the voltage range of 3.5–4.2 V, while in the discharge process, the two voltage plateaus become almost combined. This phenomenon can be illustrated by the existence of the electroactive ferrocene couple, charge–discharge behaviours of which are not in complete consistency with the triphenylamine units.

The cycling stability of the as-prepared polymers as cathode materials of Li-ion batteries is also examined, as shown in Fig. 6. It is found that both PTPAFc and PTPAn electrodes show a similar cycling performance after 30 cycles, which is decided by the nature of the organic-based material electrode. Moreover, the cycling stability of PTPAFc is even poorer than that of PTPAn at initial cycles, which is possibly due to the unstable nature of the prepared linear polymer compared to the crosslinking PTPAn during the charge–discharge process.

We further investigate the charge–discharge properties for the PTPAFc and PTPAn electrodes at various rates and Fig. 7 shows the rate and cycling performances of the polymer electrodes at different current rates of 50, 100, 300 and  $500 \text{ mA g}^{-1}$ , respectively, during the whole test of 50 cycles. Compared with parent PTPAn, PTPAFc electrodes display an obviously improved rate capability and the flat plateau curve of charge–discharge. As shown in Fig. 7(a), with an enhanced current rate from 50 to  $500 \text{ mA g}^{-1}$ , the corresponding reduction capacity for PTPAFc is only about 10.3%. Comparatively, the discharge capacities of PTPAn decreases seriously with an increase of current rate. The improved rate capability can be ascribed to the serious molecular torsion between neighbouring triphenylamines in the PTPAn molecule, which is effectively relieved by the introduction of ferrocene as the termination couple, which makes the PTPAFc main chain as a chainlike molecular structure and benefits from charge carrier transportation in the polymer molecule. In addition, the reduced crosslinking density of PTPAn, as well as a tiny particle morphology, will be convenient for the Li<sup>+</sup> ion insertion–extraction process during the charge–discharge process, which is also responsible for the high rate capability.

Fig. 7(b) further presents the charge–discharge profiles of the PTPAFc electrode at various current rates of 50, 100, 300 and  $500 \text{ mA g}^{-1}$ . Even at a rate as high as  $500 \text{ mA g}^{-1}$ , the PTPAFc electrode still displays an obviously stable voltage plateau,

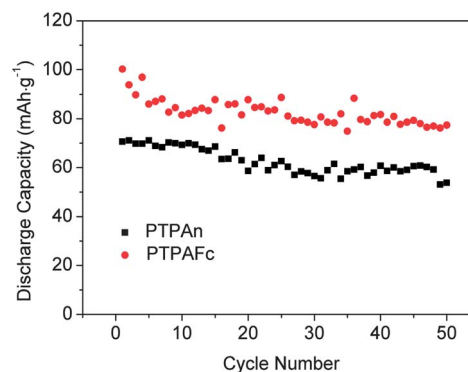


**Fig. 6** Cycling stability of the polymer electrodes material at a constant current of  $20 \text{ mA g}^{-1}$  between 2.5 and 4.2 V in  $\text{LiPF}_6 \text{ EC/DMC}$  (v/v, 1 : 1) electrolyte versus Li/Li<sup>+</sup>.

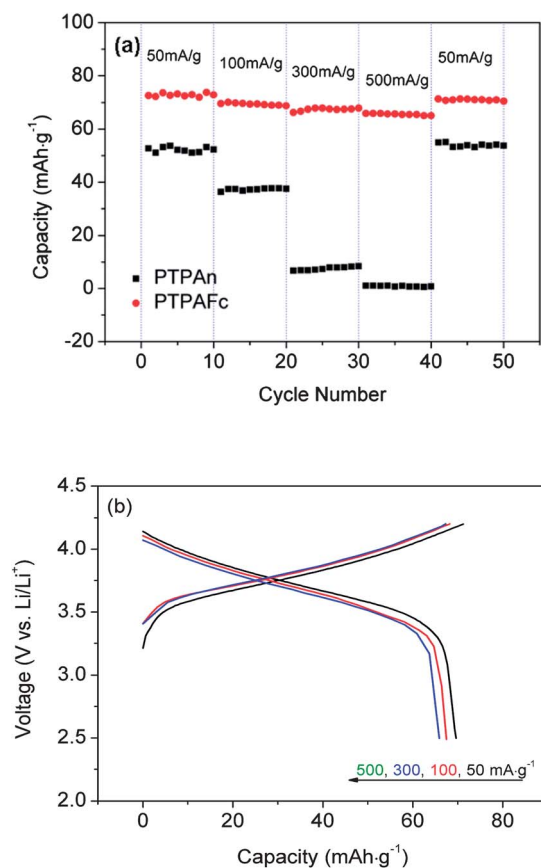


**Fig. 7** (a) The rate and cycling performances, (b) charge–discharge profiles of the polymer electrodes at voltages from 2.5–4.2 V at various current rates of 50, 100, 300 and 500 mA g<sup>-1</sup>.

implying that the PTPAFc electrodes have a lower polarization during the charge–discharge process. This further implies the superior rate capability of PTPAFc electrodes. In addition, it can be seen that the coulombic efficiency at increasing current rates is obviously improved compared to that of the initial cycle (69.0%) and reaches 95.6%, 96.6%, 97.9% and 98.9% at current rates of 50, 100, 300 and 500 mA g<sup>-1</sup> respectively.

#### 4. Conclusions

A novel linear triphenylamine derivative (TPAFc) has been successfully synthesized by the introduction of a ferrocene couple and the polymers were then prepared by chemical oxidation polymerization. Using a lithium ion half-cell method, we comparably investigated the electrochemical properties for the PTPAn and PTPAFc-based cathode. Both the introduction of the electroactive ferrocene group and the relieving of the cross-linking structure by the produced linear structure of the conducting PTPAFc were attributed to the enhancement of the capacity and rate capability of the electrode. Especially, the

PTPAFc cathode retained over 89.7% of the initial capacity with a ten times increase in the current from 50 to 500 mA g<sup>-1</sup>, which was obviously improved compared to that of the PTPAn. The improved performance of the PTPAFc-based composite cathodes made it a good candidate for the potential applications in organic lithium ion batteries.

#### Acknowledgements

The authors gratefully thank the National Natural Science Foundation of China (NSFC, no. 51003095, no. 51103132) and the Research on Public Welfare Technology Application Projects of Zhejiang Province, China (2010C31121) for financial support. This work also was supported by the analysis and testing foundation of Zhejiang University of Technology.

#### Notes and references

- 1 P. Philippe and D. Franck, *Energy Environ. Sci.*, 2011, **4**, 2003.
- 2 J. M. Tarascon and M. Armand, *Nature*, 2001, **414**(6861), 359.
- 3 M. Armand and J. M. Tarascon, *Nature*, 2008, **451**(7179), 652.
- 4 F. Y. Cheng, J. Liang, Z. L. Tao and J. Chen, *Adv. Mater.*, 2011, **23**(15), 1695.
- 5 L. Taberna, S. Mitra, P. Poizot, P. Simon and J. M. Tarascon, *Nat. Mater.*, 2006, **5**, 567.
- 6 M. Morcrette, P. Rozier, L. Dupont, E. Mugnier, L. Sannier, J. Galy and J. M. Tarascon, *Nat. Mater.*, 2003, **2**, 755.
- 7 N. Du, H. Zhang, B. D. Chen, J. B. Wu, X. Y. Ma, Z. H. Liu, Y. Q. Zhang, D. R. Yang, X. H. Huang and J. P. Tu, *Adv. Mater.*, 2007, **19**, 4505.
- 8 P. Novák, K. Müller, S. V. Santhanam and O. Hass, *Chem. Rev.*, 1997, **97**, 207.
- 9 K. S. Park, S. B. Schougaard and J. B. Goodenough, *Adv. Mater.*, 2007, **19**, 848.
- 10 Y. Su, Y. Niu, Y. Xiao, M. Xiao, Z. Liang and K. Gong, *J. Polym. Sci., Part A: Polym. Chem.*, 2004, **42**, 2329.
- 11 T. Suga, H. Konishi and H. Nishide, *Chem. Commun.*, 2007, 1730.
- 12 J. Qu, T. Katsumata, M. Satoh, J. Wada and T. Masuda, *Polymer*, 2009, **50**(2), 391.
- 13 K. Tamura, N. Akutagawa, M. Satoh, J. Wada and T. Masuda, *Macromol. Rapid Commun.*, 2008, **29**, 1944.
- 14 M. Yao, H. Senoh, T. Sakai and T. Kiyobayashi, *J. Power Sources*, 2012, **202**, 364.
- 15 M. Yao, H. Senoh, S. Yamazaki, Z. Siroma, T. Sakai and K. Yasuda, *J. Power Sources*, 2010, **195**, 8336.
- 16 J. K. Feng, Y. L. Cao, X. P. Ai and H. X. Yang, *J. Power Sources*, 2008, **177**, 199.
- 17 U. Mitschke and P. Bauerle, *J. Mater. Chem.*, 2000, **10**, 1471.
- 18 M. E. Roberts, D. R. Wheeler, B. B. McKenzie and C. B. Bruce, *J. Mater. Chem.*, 2009, **19**, 6977.
- 19 T. Saji, Y. Maruyama and S. Aoyagui, *J. Electroanal. Chem.*, 1978, **86**, 219.
- 20 J. Irena, B. Stanley, J. Angela and H. A. Robert, *J. Solid State Electrochem.*, 2004, **8**, 503.
- 21 T. Morikita and T. Yamamoto, *J. Organomet. Chem.*, 2001, **637**, 809.
- 22 T. Yamamoto, T. Morikita, T. Maruyama, K. Kubota and M. Katada, *Macromolecules*, 1997, **30**, 5390.
- 23 H. X. Qiu, Z. Y. Wang and Z. J. Shi, *Acta Phys.-Chim. Sin.*, 2007, **23**(9), 145.
- 24 W. Z. Zhang, X. W. Kan and S. F. Jiao, *J. Appl. Polym. Sci.*, 2006, **102**(6), 5633.